Eur. Phys. J. D (2019) 73: 77
https://doi.org/10.1140/epjd/e2019-90535-0

THE EUROPEAN PHYSICAL JOURNAL D

Regular Article

Isolated attosecond pulses of μJ energy via coherent Thomson-backscattering, driven by a chirped laser pulse*

Szabolcs Hack[1,2,a], Zoltán Tóth[2], Sándor Varró[1,3], and Attila Czirják[1,2]

[1] ELI-ALPS, ELI-HU Non-Profit Ltd., H-6720 Szeged, Dugonics tér 13, Hungary
[2] Department of Theoretical Physics, University of Szeged, H-6720 Szeged, Tisza L. krt. 84-86, Hungary
[3] Wigner Research Center for Physics, SZFI, H-1525 Budapest, PO Box 49, Hungary

Received 30 September 2018 / Received in final form 28 January 2019
Published online 10 April 2019

Abstract. New theoretical and numerical results are presented regarding isolated attosecond XUV – soft X-ray pulses, that can be generated by Thomson-backscattering of a high-intensity single-cycle near-infrared laser pulse on a suitable nanobunch of MeV electons. A simple approximate formula is derived for the cut-off frequency of the collective radiation spectrum, which is then employed to find the length of the nanobunch which emits an isolated pulse of 16 as length. Detailed analysis of the spectral, temporal and spatial features of this attosecond pulse is given. It is also shown that the 100 nJ pulse energy, corresponding to 2.1×10^{18}W/cm^2 peak intensity of the laser pulse, can be increased to reach the μJ pulse energy both by increasing the intensity or by setting a suitable down-chirp of the laser pulse.

1 Introduction

Attosecond pulses of "light", usually in the XUV – soft X-ray spectral range, allow us to experimentally access the real time electron dynamics in atoms, molecules and solids [1]. At present, high-order-harmonic generation in noble gas samples is the most reliable method to generate attosecond XUV pulses [2,3], which, however, has its limitations both in pulse length and intensity.

Thomson-backscattering of an intense laser pulse on a relativistic electron bunch is a well-known source of (hard) X- and gamma-ray radiation [4–10]. In our earlier works [11,12], we already showed that Thomson-backscattering of a linearly polarized near-infrared few-cycle laser pulse on a suitable electron bunch may provide isolated attosecond pulses also in the XUV – soft X-ray spectral range, including the 2.33–4.37 nm water window. According to our calculations, these attosecond pulses are almost linearly polarized and extremely well collimated, and their carrier-envelope phase difference (CEP) is locked to that of the laser pulse.

The availability of suitable electron bunches is crucial for attosecond pulse generation via Thomson-backscattering. Based on pioneering experiments [13,14] and enlightening simulations [15], the state of the art methods are (i) velocity bunching, producing bunches of pC charge, MeV energy, sub-10 fs pulse length [9,16,17], (ii) bunch compression, providing bunches of 2 as duration and 5.2 MeV energy [18], (iii) laser-wakefield acceleration, yielding quasi-monoenergetic, fs or sub-fs electron bunch trains [19–21], or even an isolated electron bunch [22] of 10–100 pC charge (i.e. 10^7-10^8 electrons) and of few to few hundred MeV energy. The radiation emission by laser-generated electron nanobunches has also been studied in [23–25], where the authors also predicted the generation of extremely dense electron bunches in the few 10–100 nm length range having a few MeV energy.

Based on these developments, relativistic electron nanobunches with parameters used in the present paper are expected to be available in the near future. In order to investigate the Thomson scattering of a near infrared (NIR) few-cycle chirped laser pulse on such an nanobunch, we start from the Newton–Lorentz equations. We compute and analyse the collective radiation and we also give an approximate analytic formula for its cut-off frequency. We show that the energy of the attosecond pulse can be increased from the nJ to the μJ energy range by increasing the intensity or by setting a suitable value for the chirp of the driving laser pulse.

2 Theoretical model

Let us assume a coordinate system in which the driving laser pulse propagates along the z axis and it is linearly polarized along the x axis. First, we consider a single electron only, which moves initially in the $-z$ direction, i.e.

* Contribution to the Topical Issue "Many Particle Spectroscopy of Atoms, Molecules, Clusters and Surfaces (2018)", edited by Károly Tőkési, Béla Paripás, Gábor Pszota, and Andrey V. Solov'yov.

[a] e-mail: Szabolcs.Hack@eli-alps.hu

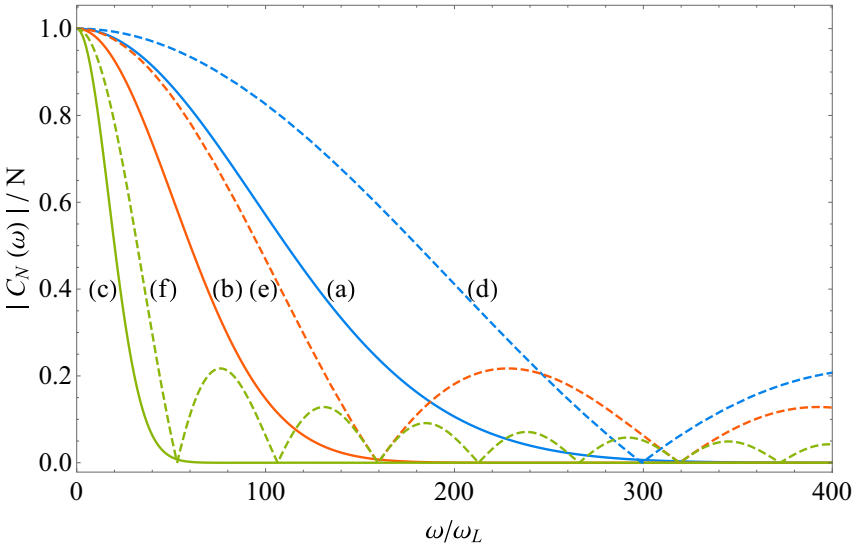

Fig. 1. Frequency dependence of the magnitude of the coherence factor C_N (normalized to N) along the backscattering direction. Curves (a)–(c) correspond to realistic electron nanobunches with stochastic electron positions having a Gaussian distribution in the longitudinal direction. Curves (d)–(f) correspond to artificial electron nanobunches with an equidistant spacing of electrons. The longitudinal length of the equidistant bunch is set equal to the full width (2 standard deviations) of the longitudinal Gaussian distribution of the realistic bunch for corresponding curves (a) and (d): $L_{\mathrm{bunch}} = 2.66\,\mathrm{nm}$, (b) and (e): $L_{\mathrm{bunch}} = 5\,\mathrm{nm}$, (c) and (f): $L_{\mathrm{bunch}} = 15\,\mathrm{nm}$. All other parameters are the same for all curves.

we are in head-on collision scenario. We model the electric field of the laser pulse, $\mathbf{E} = (E_x, 0, 0)$, with the usual sine-squared envelope:

$$E_x(\theta) = E_0 \sin^2\left(\frac{\omega_L \theta}{2n_c}\right) \cos\left((\omega_L + k\theta)\theta - \varphi_0\right), \quad (1)$$

where E_0 is the amplitude, ω_L is the angular frequency, n_c is the number of optical cycles in the pulse, k is the chirp parameter, φ_0 is the CEP and $\theta = t - \boldsymbol{n}_L \cdot \mathbf{r}/c$ is the wave argument of the laser pulse at position $\mathbf{r}$, with $\boldsymbol{n}_L$ denoting the unit vector pointing in the propagation direction. We assume uniform transverse beam profile in order to have the advantage of analytic treatment. For detailed numerical investigations of the effects of the transverse beam profile see references [26–28].

The Newton–Lorentz equations govern the motion of a relativistic electron with charge e and mass m during its interaction with the laser pulse as

$$m\frac{d\mathbf{u}}{d\tau} = \frac{e}{c}\left[u^0 \mathbf{E}(\theta) + \boldsymbol{n}_L\left(\mathbf{u}\cdot\mathbf{E}(\theta)\right) - \mathbf{E}(\theta)\left(\boldsymbol{n}_L\cdot\mathbf{u}\right)\right], \quad (2)$$

$$m\frac{du^0}{d\tau} = \frac{e}{c}\mathbf{E}(\theta)\cdot\mathbf{u}, \quad (3)$$

where $\left(u^0, \mathbf{u}\right) = (\gamma c, \gamma \mathbf{v})$ is the four-velocity, $\gamma \equiv \left(1 - |\mathbf{v}|^2/c^2\right)^{-1/2}$ is the Lorentz-factor and $d\tau = dt/\gamma$ is the proper time element of the electron. In equation (3) we have made use of the $\mathbf{B} = \boldsymbol{n}_L \times \mathbf{E}/c$, connecting the magnetic induction and the electric field strength of a plane wave. As it is well known, the equations of motion (2)–(3) have a general analytic solution [29–31] and in [12] we determined an explicit particular solution of equations (2)–(3) for a laser pulse corresponding to equation (1) with $k = 0$. Using this solution, we are able to evaluate the spectrum of radiation emitted by an electron, which is given in the far-field by the following formula [32]:

$$\mathbf{E_1}(\omega) = \frac{e}{c}\frac{e^{i\omega R_0/c}}{4\pi\epsilon_0 R_0}\int_{-\infty}^{\infty} \frac{\boldsymbol{n}\times\left[(\boldsymbol{n}-\beta)\times\dot{\beta}\right]}{(1-\boldsymbol{n}\cdot\beta)^2} e^{i\omega(t-\mathbf{n}\cdot\mathbf{r}(t)/c)}dt, \quad (4)$$

where R_0 is the distance of the observation point, $\boldsymbol{n}$ is the unit vector pointing towards the observer, $\beta = \mathbf{v}/c$ and $\dot{\beta}$ are the normalized velocity and acceleration, respectively.

Then we can generalize equation (4) to describe the collectively emitted Thomson-backscattered radiation of an ideal electron bunch with the help of the coherence factor (sometimes called also relativistic form factor) [33,34]:

$$C_N(\omega) = \sum_{k=1}^{N} \exp\left[i\omega\left(t_k(\theta_0) - \frac{\boldsymbol{n}\cdot\mathbf{r}_k(\theta_0)}{c}\right)\right], \quad (5)$$

which takes into account the effect of the different initial positions of the electrons on the collectively emitted spectrum of N electrons as:

$$\mathbf{E}_N(\omega) = C_N(\omega)\,\mathbf{E_1}(\omega). \quad (6)$$

Since the frequency-dependence of the coherence factor equation (5) influences the spectrum of the collective radiation in an essential way [12], we plot the magnitude of $C_N(\omega)$ in Figure 1 for electron nanobunches of different lengths. For each length, we plot $|C_N(\omega)|$ both for a realistic electron nanobunch with stochastic electron positions characterized by a uniform distribution in the transverse direction and a Gaussian distribution in the longitudinal direction (solid lines), and for a rather artificial electron nanobunch with an equidistant spacing of

electron positions (dashed lines). The number of electrons and the transverse size is the same for the bunches, and the longitudinal length of the equidistant bunch is equal to the full width (i.e. 2 standard deviations) of the longitudinal Gaussian distribution of the realistic bunch. As it is expected, $|C_N(\omega)|$ decreases faster with increasing angular frequency in the case of the realistic nanobunch, and it does not exhibit the series of higher frequency peaks as it does in case of the nanobunch with equidistant electrons. However, it is interesting that the first zero of $|C_N(\omega)|$ of the equidistant nanobunch is a good approximation for the cut-off frequency of $|C_N(\omega)|$ of the corresponding realistic nanobunch.

Based on equation (5), we can easily obtain a simple approximate expression for this cut-off frequency (ω_c) of the constructive interference of the Thomson-backscattered radiation by an electron nanobunch. Here we consider only the on-axis radiation by setting $\boldsymbol{n} = (0, 0, -1)$. From references [11,33] we know that one has to transform the usual initial conditions, which are valid in a lab-frame (i.e. on a space-like hyper-surface), to the light-like hyper-surface due to the use of the wave argument θ in equations (2)–(3). Thus $ct_k(\theta_0 = 0)$ and $z_k(\theta_0 = 0)$ take the following form:

$$ct_k(\theta_0 = 0) = z_k(\theta_0 = 0) = \frac{z_k(t_0 = 0)}{(1 + \frac{|v_z(t_0=0)|}{c})}. \quad (7)$$

Making use of the assumed equidistant spacing with the distance $\overline{z} = L_{\text{bunch}}/N$ between the electrons, where L_{bunch} is the length of the bunch consisting of N electrons, and using the connection $|v_z(t_0 = 0)| = c\sqrt{1 - 1/\gamma_0^2}$ between the initial Lorentz-factor and the velocity, we obtain from equation (5) the following:

$$C_N(\omega) = \sum_{k=0}^{N-1} \left(\exp\left[i \frac{\omega}{c} \frac{2}{1 + \sqrt{1 - 1/\gamma_0^2}} \frac{L_{\text{bunch}}}{N-1} \right] \right)^k. \quad (8)$$

With the well known exponential sum formula, we get the magnitude of the coherence factor as:

$$|C_N(\omega)| = \left| \frac{\sin\left(\frac{\omega}{c} \frac{1}{1+\sqrt{1-1/\gamma_0^2}} \frac{L_{\text{bunch}}}{N-1} N \right)}{\sin\left(\frac{\omega}{c} \frac{1}{1+\sqrt{1-1/\gamma_0^2}} \frac{L_{\text{bunch}}}{N-1} \right)} \right|. \quad (9)$$

For a high-density nanobunch (i.e. $N \gg 1$ and $L_{\text{bunch}} < \lambda_{\text{L}}$), the sine in the denominator of equation (8) can be approximated by its argument. Then we obtain the following expression for the first zero of $|C_N(\omega)|$:

$$\omega_c = c \left(1 + \sqrt{1 - 1/\gamma_0^2} \right) \frac{\pi}{L_{\text{bunch}}}. \quad (10)$$

According to the discussion of the curves of Figure 1, this formula above gives the approximate cut-off frequency of an ideal high-density electron nanobunch having a realistic stochastic electron distribution. It depends only weakly on the initial Lorentz-factor γ_0, but it is very sensitive to the length of the bunch, L_{bunch}.

3 Emitted radiation spectra and pulse shapes

Applying the considerations and results of the previous section, we evaluate now the radiation spectrum emitted by an electron and then by an electron bunch, moving according to the solution of equations (2)–(3). We assume a realistic almost single-cycle (at FWHM) cosine-type laser pulse by setting $n_c = 3$, $k = 0$ and $\varphi_0 = 0$, with a carrier wavelength of $\lambda_L = 800\,\text{nm}$ and a dimensionless vector potential of $a_0 = 1$, corresponding to a peak electric field of ca. $4 \times 10^{12}\,\text{V/m}$ (i.e. $a_0 = 8.5 \times 10^{-10} \lambda\,[\mu\text{m}] \sqrt{I_0\,[\text{W/cm}^2]}$). We show the resulting back-scattered single electron radiation spectrum in Figure 2 for the initial Lorentz-factor (γ_0) of 10, along the directions $\mathbf{n}$ in the $x - z$ plane defined by the indicated polar angles (i.e. along and very close to the direction of the electron's initial velocity at 180°). We set the polar angle range in Figures 2–4 to the usually expected beam divergence of $1/\gamma_0$. We plot the spectrum of the dominant x component of the electric field. The single electron spectrum on Figure 2 is more sensitive with respect to the change of the polar angle than in case of a long laser pulse. Furthermore, the nearly single-cycle length of the driving laser pulse causes further spectral broadening compared to the long laser pulse or to the continuous wave limit [35–38].

Based on the single electron spectrum and on equation (5), we can now consider the collective radiation of an electron bunch. According to equation (10), we need an electron bunch with a length of 2.66 nm in order to generate a broad collective spectrum, e.g. constructive interference up to $300\omega_L$. This so called electron nanobunch is well known in the literature, it consists typically of 10^5–10^8 electrons and has its longitudinal size in the 1–100 nm range. The assumed initial Lorentz-factor, corresponding to 5.2 MeV energy, and the calculated bunch length are close to the simulation results of Naumova et al. [15] and to the predictions of Sell and Kärtner [18]. In our calculations, we assume a bunch of $N = 10^8$ electrons with negligible energy spread, its distribution is uniform with a size of 800 nm ($= \lambda_L$) in the transverse direction, while its distribution is Gaussian with a size of 2.66 nm (2 standard deviation) in the longitudinal direction. Several experimental [13,14,19–22] and simulation results [39–41] suggest that these nanobunch parameters are within reach experimentally in the near future.

The applied parameters allow us to treat the electron bunch as an ideal bunch. That is, we neglect the radiation reaction because the characteristic time of the energy loss by radiation reaction [34,42] is five orders of magnitude larger than the interaction time. We also neglect the electron-electron interaction since the Coulomb-force between the electrons is three orders of magnitude smaller than the Lorentz-force due to the laser pulse for $a_0 = 1$. The effect of the energy spread of 0.1% or less is also negligible for these parameters. The nonzero transverse emittance of the bunch, which depends on the transverse velocity components, does not modify the results because the dominant terms of the trajectories include the longitudinal component of the velocity only. Additionally, we

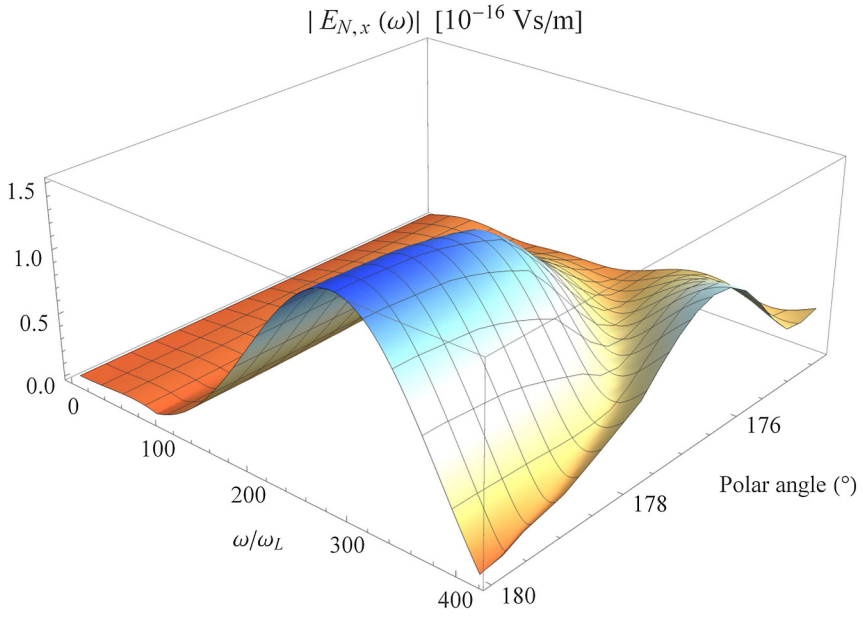

Fig. 2. Polar angle dependence of the Thomson-backscattering spectrum, radiated by a single electron, having an initial energy of 5.2 MeV (corresponding to $\gamma_0 = 10$). The driving laser pulse is an almost single-cycle cosine-type laser pulse of sine-squared envelope. We plot the dominant x-component of the electric field along the propagation directions in the $x - z$ plane near the backscattering direction (at 180°). Other parameters: $\lambda_L = 800\,\text{nm}$, $n_c = 3$, $k = 0$, $\varphi_0 = 0$, $a_0 = 1$, $R_0 = 2\,\text{m}$.

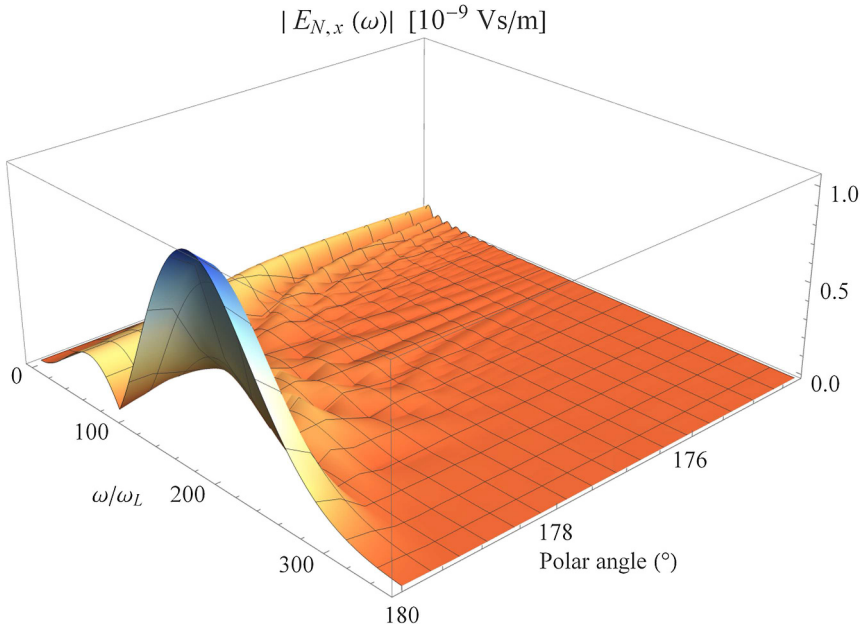

Fig. 3. Polar angle dependence of the Thomson-backscattering spectrum, radiated collectively by an nanobunch of 10^8 electrons described in the main text. Other parameters are the same as for Figure 2.

investigate the backscattered radiation, very close to 180°, which further suppresses the effect of the transverse emittance in equation (4).

Next we show the polar angle dependence of the spectral amplitude of the collective radiation in Figure 3, computed on the basis of equation (6) for the bunch parameters mentioned above. The collective nature of the radiation causes a narrower radiation cone compared to Figure 2, because of the sensitive dependence of the coherence factor on the polar angle, which was investigated in [12].

We show the polar angle resolved temporal pulse shape of the collective radiation in Figure 4, based on the inverse Fourier transform of the data of Figure 3. The resulting attosecond pulse has only two oscillations and its length at FWHM is 16 as. In a distance of 2 m from interaction region, the peak intensity is $6.21 \times 10^9\,\text{W/cm}^2$ and

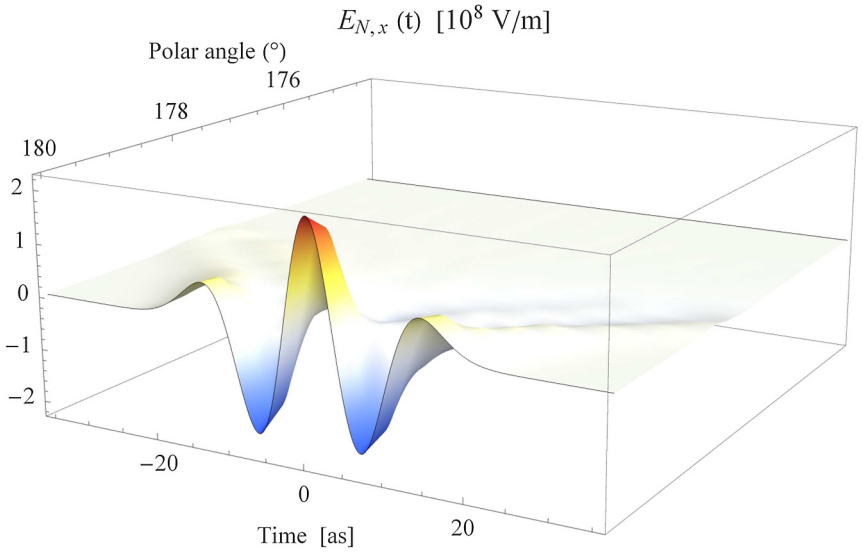

Fig. 4. Temporal and spatial pulse shape of the isolated attosecond pulse, computed from the spectrum on Figure 3. We note that the emitted pulse has azimuthal symmetry.

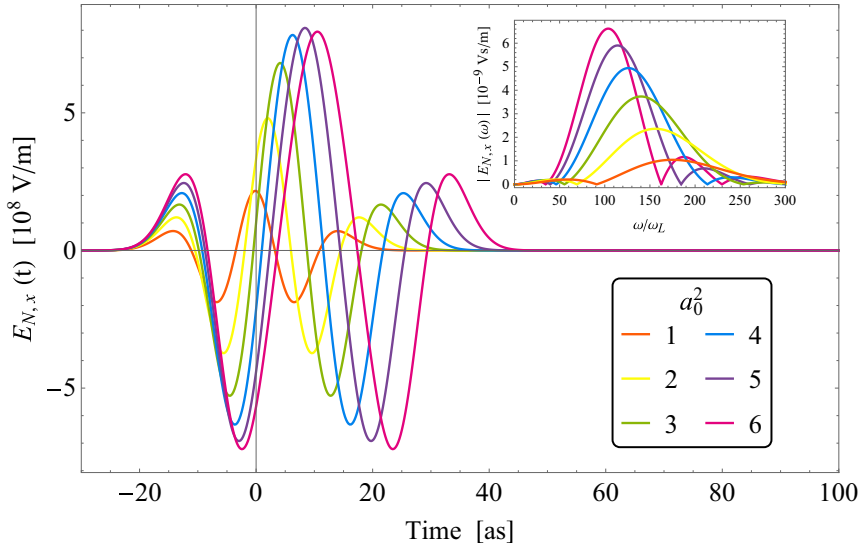

Fig. 5. Temporal pulse shapes of the isolated attosecond pulses along the backscattering direction (at 180°) for indicated values of the squared normalized vector potential (a_0^2) for the single-cycle cosine-type laser pulse. The inset shows the corresponding spectra. The electron bunch parameters are the same as for Figure 3.

the average intensity is 1.31×10^9 W/cm^2, giving a pulse energy of 99 nJ.

A seemingly obvious way to increase the energy and the intensity of the attosecond pulse is to increase the intensity of the NIR pulse. We plot the temporal shapes of the resulting attosecond pulses at 180° in Figure 5, corresponding to a_0^2 values in the range of 1–6, and we plot the corresponding spectra in the inset using the same electron bunch parameters as before.

Based on the collective spectra, we see that, although the intensity of the driving pulse is in the nonlinear regime, only the linear peaks of the single electron spectra contribute to the collective radiation, owning to the properties of the coherence factor. Since these peaks, besides gaining more spectral intensity, get also red-shifted and narrowed with increasing laser intensity, the resulting pulses contain much more energy and become somewhat longer.

Figure 5 shows that the intensity and the energy of the attosecond pulse increase non-linearly with increasing intensity of the driving laser pule up to a certain intensity limit which depends on the parameters of the bunch, the central wavelength and the pulse length of the driving laser field. E.g. for $a_0^2 = 3$, the peak intensity is 6.15×10^{10} W/cm^2 and the average intensity is 2.62×10^{10} W/cm^2, already giving a pulse energy of ca. 500 nJ. For $a_0^2 = 5$, this effect is much stronger, the pulse energy increases with a factor of 10, reaching already the μJ energy range. However, further increase of the NIR intensity does not cause any increase of the intensity or the energy of the attosecond pulse.

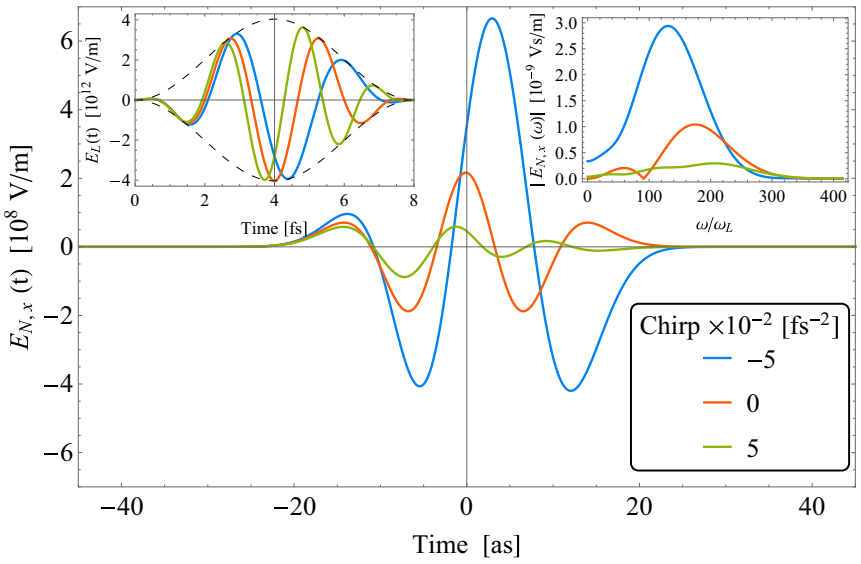

Fig. 6. Temporal pulse shapes of the isolated attosecond pulses, obtained by nonlinear Thomson-backscattering at 180°, for the indicated values of chirp parameter (k) for the cosine-type laser pulse. The insets show the incoming NIR pulse shapes (left) and the corresponding collective spectra (right) for different values of k. The electron bunch parameters are the same as for Figure 3.

High-intensity laser pulses are usually chirped, which provides an additional control parameter for the Thomson-backscattering process. It is thus interesting to explore how the chirp of the driving laser pulse affects the emitted collective radiation spectrum and the resulting attosecond pulse. To our best knowledge, this question was not investigated for coherent Thomson-backscattering previously. We note that for nonzero k, the explicit analytic solution of the equations of motion (2)–(3) requires some further approximations, therefore we use a numerical solution instead. We show the resulting attosecond pulse shapes in Figure 6 for two nonzero values of the chirp parameter k of the laser pulse, in comparison with the case of zero chirp. The left inset of Figure 6 plots the corresponding driving laser pulses, while the right inset shows the corresponding collective spectra. The result is somewhat counter-intuitive, since one would expect that the energy of the attosecond pulse increases with the energy of the driving laser pulse (since a laser pulse with positive chirp contains more energy). In contrast, our results show that the intensity and the energy of the attosecond pulse increase if the driving laser pulse is down-chirped. E.g. for $k = -5 \times 10^{-2}\text{fs}^{-2}$, the energy of the attosecond pulse can be increased up to 1 μJ, which is an order of magnitude larger than in the case of zero chirp. This can be explained again by the collective nature of radiation. The down-chirp causes a quiet decrease and a significant red-shift on the peaks of the single-electron spectrum, which is much more favourable to the constructive interference of the electrons' radiation than the opposite process caused by the up-chirp. This prediction about the energy dependence of the attosecond pulse on the chirp of the driving laser pulse could be easily verified experimentally. Note also that the pulse length remains the original 16 as, although the pulse-shape changes.

4 Summary and conclusions

Our theoretical investigations show that the Thomson-backscattering of a NIR laser pulse on a suitable relativistic electron nanobunch is a promising source of an isolated attosecond XUV – soft X-ray pulse, having advantageous features. Based on the analysis of the coherence factor, we derived a simple formula for the cut-off frequency of the collective radiation spectrum, which could be useful also in designing the corresponding experiments. As an example, we have shown that an nanobunch of 10^8 electrons having 5.2 MeV energy, driven by a few-fs NIR laser pulse of ca. 2.1×10^{18} W/cm^2 peak intensity, could produce an isolated attosecond pulse of 16 as pulse-length and ca. 100 nJ energy. Our results also show that the energy of the attosecond pulse can be effectively increased by increasing the intensity or by changing the chirp of the driving laser pulse: e.g. with a proper down-chirp of the laser pulse, the attosecond pulse energy could reach the μJ energy range.

Open access funding provided by ELI-HU Non-profit Ltd. The authors thank M. G. Benedict, P. Földi, Zs. Lécz, D. Papp, Cs. Tóth and Gy. Tóth for stimulating discussions. The project has been supported by the European Union, co-financed by the European Social Fund, EFOP-3.6.2-16-2017-00005. Partial support by the ELI-ALPS project is also acknowledged. The ELI-ALPS project (GOP-1.1.1-12/B-2012-000, GINOP-2.3.6-15-2015-00001) is supported by the European Union and co-financed by the European Regional Development Fund.

Author contribution statement

Sándor Varró initiated the project and supervised it with Attila Czirják. Szabolcs Hack performed the analytic

calculations and the numerical simulations. All authors contributed to the analysis of the results and to the writing of the manuscript.

References

1. F. Krausz, M. Ivanov, Rev. Mod. Phys. **81**, 163 (2009)
2. G. Farkas, C. Tóth, Phys. Lett. A **168**, 447 (1992)
3. G. Sansone, E. Benedetti, F. Calegari, C. Vozzi, L. Avaldi, R. Flammini, L. Poletto, P. Villoresi, C. Altucci, R. Velotta, S. Stagira, S.D. Silvestri, M. Nisoli, Science **314**, 443 (2006)
4. K. Lee, Y.H. Cha, M.S. Shin, B.H. Kim, D. Kim, Phys. Rev. E **67**, 026502 (2003)
5. W. Yan, C. Fruhling, G. Golovin, D. Haden, J. Luo, P. Zhang, B. Zhao, J. Zhang, C. Liu, M. Chen, S. Chen, S. Banerjee, D. Umstadter, Nat. Photon. **11**, 514 (2017)
6. D. Kim, H. Lee, S. Chung, K. Lee, New J. Phys. **11**, 063050 (2009)
7. S.Y. Chung, M. Yoon, D.E. Kim, Opt. Express **17**, 7853 (2009)
8. M. Chen, E. Esarey, C.G.R. Geddes, C.B. Schroeder, G.R. Plateau, S.S. Bulanov, S. Rykovanov, W.P. Leemans, Phys. Rev. ST Accel. Beams **16**, 030701 (2013)
9. W. Luo, T.P. Yu, M. Chen, Y.M. Song, Z.C. Zhu, Y.Y. Ma, H.B. Zhuo, Opt. Express **22**, 32098 (2014)
10. J.X. Li, K.Z. Hatsagortsyan, B.J. Galow, C.H. Keitel, Phys. Rev. Lett. **115**, 204801 (2015)
11. S. Hack, S. Varró, A. Czirják, Nucl. Instr. Meth. Phys. Res. B. **369**, 45 (2016)
12. S. Hack, S. Varró, A. Czirják, New J. Phys. **20**, 073043 (2018)
13. C.G.R. Geddes, C. Tóth, J. van Tilborg, E. Esarey, C.B. Schroeder, D. Bruhwiler, C. Nieter, J. Cary, W.P. Leemans, Nature **431**, 538 (2004)
14. C.M.S. Sears, E. Colby, R. Ischebeck, C. McGuinness, J. Nelson, R. Noble, R.H. Siemann, J. Spencer, D. Walz, T. Plettner, R.L. Byer, Phys. Rev. ST Accel. Beams **11**, 061301 (2008)
15. N. Naumova, I. Sokolov, J. Nees, A. Maksimchuk, V. Yanovsky, G. Mourou, Phys. Rev. Lett. **93**, 195003 (2004)
16. J. Zhu, R.W. Assmann, M. Dohlus, U. Dorda, B. Marchetti, Phys. Rev. ST Accel. Beams **19**, 054401 (2016)
17. J. Maxson, D. Cesar, G. Calmasini, A. Ody, P. Musumeci, D. Alesini, Phys. Rev. Lett. **118**, 154802 (2017)
18. A. Sell, F.X. Kärtner, J. Phys. B: At. Mol. Opt. Phys. **47**, 015601 (2014)
19. K. Schmid, A. Buck, C.M.S. Sears, J.M. Mikhailova, R. Tautz, D. Herrmann, M. Geissler, F. Krausz, L. Veisz, Phys. Rev. ST Accel. Beams **13**, 091301 (2010)
20. A. Buck, M. Nicolai, K. Schmid, C.M.S. Sears, A. Svert, J.M. Mikhailova, F. Krausz, M.C. Kaluza, L. Veisz, Nat. Phys. **7**, 543548 (2011)
21. A. Buck, J. Wenz, J. Xu, K. Khrennikov, K. Schmid, M. Heigoldt, J.M. Mikhailova, M. Geissler, B. Shen, F. Krausz, S. Karsch, L. Veisz, Phys. Rev. Lett. **110**, 185006 (2013)
22. M. Heigoldt, A. Popp, K. Khrennikov, J. Wenz, S.W. Chou, S. Karsch, S.I. Bajlekov, S.M. Hooker, B. Schmidt, Phys. Rev. ST Accel. Beams **18**, 121302 (2015)
23. D. an der Brügge, A. Pukhov, Phys. Plasmas **17**, 033110 (2010)
24. A.A. Gonoskov, A.V. Korzhimanov, A.V. Kim, M. Marklund, A.M. Sergeev, Phys. Rev. E **84**, 046403 (2011)
25. M. Cherednychek, A. Pukhov, Phys. Plasmas **23**, 103301 (2016)
26. C.A. Brau, Phys. Rev. ST Accel. Beams **7**, 020701 (2004)
27. P.A. Golovinski, E.A. Mikhin, J. Exp. Theor. Phys. **113**, 545 (2011)
28. O.E. Vais, S.G. Bochkarev, V.Y. Bychenkov, Plasma Phys. Rep. **42**, 818 (2016)
29. N.D. Sengupta, Bull. Math. Soc. **41**, 187 (1949)
30. E.M. McMillan, Phys. Lett. **79**, 498 (1950)
31. I.I. Goldman, Phys. Lett. **8**, 103 (1964)
32. J.D. Jackson, *Classical Electrodynamics*, 4th edn. (Wiley New York, 1999)
33. S. Varró, F. Ehlotzky, Z. Phys. D: At., Mol. Clusters **22**, 619 (1992)
34. S. Corde, K. Ta Phuoc, G. Lambert, R. Fitour, V. Malka, A. Rousse, A. Beck, E. Lefebvre, Rev. Mod. Phys. **85**, 1 (2013)
35. E. Esarey, S.K. Ride, P. Sprangle, Phys. Rev. E **48**, 3003 (1993)
36. F.V. Hartemann, A.L. Troha, N.C. Luhmann, Z. Toffano, Phys. Rev. E **54**, 2956 (1996)
37. A.G.R. Thomas, Phys. Rev. ST Accel. Beams **13**, 020702 (2010)
38. S.G. Rykovanov, C.G.R. Geddes, J.L. Vay, C.B. Schroeder, E. Esarey, W.P. Leemans, J. Phys. B: At. Mol. Opt. Phys. **47**, 234013 (2014)
39. V.V. Kulagin, V.A. Cherepenin, M.S. Hur, H. Suk, Phys. Rev. Lett. **99**, 124801 (2007)
40. F.Y. Li, Z.M. Sheng, Y. Liu, J. Meyer-ter Vehn, W.B. Mori, W. Lu, J. Zhang, Phys. Rev. Lett. **110**, 135002 (2013)
41. L.J. Wong, B. Freelon, T. Rohwer, N. Gedik, S.G. Johnson, New J. Phys. **17**, 013051 (2015)
42. L. Landau, E. Lifshitz, in *The Classical Theory of Fields*, *Course of Theoretical Physics*, 4th edn. (Pergamon, 1975), Vol. 2